Karbala International Journal of Modern Science

Manuscript 3433

Synthesis of Nitrogen-Enriched 3D Graphene Foam for Electrochemical Sensing of Hydrogen Peroxide (H_2O_2)

Bhargavi Dronavalli

Madhava Rao Vallabhaneni

Jatla Murali Prakash

Deepti Kolli

Dandamudi Srilaxmi

Synthesis of Nitrogen-Enriched 3D Graphene Foam for Electrochemical Sensing of Hydrogen Peroxide (H_2O_2)

Abstract

In this work, A simple hydrothermal process was utilized to create 3D-foam-type Nitrogen-doped graphene (NDG). The synthesized material was characterized using a range of physicochemical characterization techniques. These techniques confirm that nitrogen is successfully incorporated into the carbon network, resulting in NDG. Cyclic voltammetry (CV) investigation demonstrated that NDG-modified glassy carbon electrode (NDG/GCE) displayed finite charge transfer properties against typical redox systems. NDG/GCE is identified as a simple, facile, and efficient electrocatalyst material for the estimation of hydrogen peroxide (H_2O_2). From CV analysis, it is revealed that NDG/GCE can produce a signal for electrochemical quantification of H_2O_2 at an applied overpotential of -0.15 V. The GCE and GO/GCE were unable to respond to the estimation of H_2O_2. However, NDG/GCE exhibited finite sensitivity and linearity for a concentration range of 0.5 µM to 16 µM. This was examined using amperometric protocols, where the detection limit and observed sensitivity for NDG/GCE are 0.3 µM and 0.34 µA/µM respectively. The selectivity study has further revealed that the electrode can produce a signal selectively towards H_2O_2 in the presence of other possible foreign molecules. In conclusion, the electrode is determined to be stable for 15 days concerning the electrochemical estimation of H_2O_2 with the aid of stability investigations

Keywords

Nitrogen-doped graphene; Hydrogen Peroxide; Amperometry; Limit of detection

RESEARCH PAPER

Synthesis of Nitrogen-enriched 3D Graphene Foam for Electrochemical Sensing of Hydrogen Peroxide (H_2O_2)

Bhargavi Dronavalli [a], Madhava R. Vallabhaneni [b,**], Jatla M. Prakash [c], Deepti Kolli [c,*], Dandamudi Srilaxmi [d]

[a] Department of Chemistry, Acharya Nagarjuna University, Guntur 522 510, Andhra Pradesh, India
[b] Department of Chemistry (Recognized as Research Centre by ANU), Bapatla Engineering College (Autonomous), Bapatla 522102, India
[c] Department of Chemistry, Koneru Lakshmaiah Education Foundation, Greenfields, Vaddeswaram, Guntur 522502, Andhra Pradesh, India
[d] Department of Chemistry, Parvathaneni Brahmayya Siddhartha College of Arts & Science, Vijayawada-10, Andhra Pradesh, India

Abstract

In this work, A simple hydrothermal process was utilized to create 3D-foam-type Nitrogen-doped graphene (NDG). The synthesized material was characterized using a range of physicochemical characterization techniques. These techniques confirm that nitrogen is successfully incorporated into the carbon network, resulting in NDG. Cyclic voltammetry (CV) investigation demonstrated that NDG-modified glassy carbon electrode (NDG/GCE) displayed finite charge transfer properties against typical redox systems. NDG/GCE is identified as a simple, facile, and efficient electrocatalyst material for the estimation of hydrogen peroxide (H_2O_2). From CV analysis, it is revealed that NDG/GCE can produce a signal for electrochemical quantification of H_2O_2 at an applied overpotential of −0.15 V. The GCE and GO/GCE were unable to respond to the estimation of H_2O_2. However, NDG/GCE exhibited finite sensitivity and linearity for a concentration range of 0.5 μM−16 μM. This was examined using amperometric protocols, where the detection limit and observed sensitivity for NDG/GCE are 0.3 μM and 0.34 μA/μM respectively. The selectivity study has further revealed that the electrode can produce a signal selectively towards H_2O_2 in the presence of other possible foreign molecules. In conclusion, the electrode is determined to be stable for 15 days concerning the electrochemical estimation of H_2O_2 with the aid of stability investigations.

Keywords: Nitrogen-doped graphene, Hydrogen peroxide, Amperometry, Cyclic voltammetry, Limit of detection

1. Introduction

Graphene, one of the allotropic forms of carbon, consists of orderly arranged sp^2 hybridized carbon atoms. The carbon atoms are formed as a monolayer and exist as a honeycomb structure. Since its discovery in 2004, graphene has gained attention for its outstanding properties: large surface area, strong Young's modulus, high thermal and electrical conductivity, and optical transparency [1−6]. Because of these fascinating properties, the role of graphene has become inevitable in numerous sectors of research [7]. So far, there are a plethora of procedures developed for the preparation of graphene, including chemical vapour deposition (CVD) [8], exfoliation of graphite [9], solvothermal synthesis [10], and reduction of graphene oxide (GO) [11]. Among these proposed methods, the thermal route provides the foremost advantages as follows. It is a modern, rapid technique that eliminates the use of toxic solvents. As a result, the final product will not be contaminated

Received 25 May 2025; revised 29 August 2025; accepted 2 September 2025.
Available online 3 October 2025

* Corresponding author.
** Corresponding author.
E-mail addresses: vmrgpm@gmail.com (M.R. Vallabhaneni), atluri.deepti1984@gmail.com (D. Kolli).

https://doi.org/10.33640/2405-609X.3433

[12]. In addition, the functionalization of graphene with suitable foreign materials is quite interesting to improve its electrocatalytic activity. In this regard, graphene is functionalised with various other materials like polymers, metal nanoparticles and heteroatoms like nitrogen, sulphur, oxygen etc. [13–15], and they have been identified as successful candidates in several uses that include electrochemical sensors, electronic devices, energy conversion/storage systems and electro catalysis, among others etc [16]. Particularly the nitrogen element as ideal dopant for carbon-based materials, because nitrogen have close atomic radius (0.7 Å) similar to carbon atom (0.77 Å) and higher electronegativity than carbon. These properties enhance the charge carrier mobility and create more electroactive sites in the NDG catalyst material at interface for superior electrochemical performance.

Hydrogen peroxide is used as an oxidizing agent in many reactions and is found as one of the by-products of a lot of oxidase enzymes. The role of the molecules is inevitable in various sectors like textiles, food industries, and so on [17,18]. It also regulates various biological processes, including immune cell activation and root growth in organisms. Since H_2O_2 is involved in cellular growth and apoptosis, it is one of the important chemicals in biological processes [19]. On the other hand, the transportation and storage of H_2O_2 in large excess is found to a risky, which limits its applications [20]. With the help of H_2O_2 and its derivatives, which are rich in reactive primary oxygen groups like superoxide radical ($O_2^{\bullet}$) and hydroxyl radical ($OH^{\bullet}$). Further they identified as the by-products of aerobic metabolism in the human system. Their level increases in the human system under stress. Therefore, maintaining the level of H_2O_2 is highly crucial in the human system [21–23]. The failure of this leads to several health risks like cancer, Parkinson's and Alzheimer's disease etc [24,25]. Hence, a lot of attention is being paid for synthesising efficient, reliable, highly sensitive, economical and stable catalysts and sensors for accurate quantification of H_2O_2. In this regard, several analytical protocols like spectroscopy [26], chromatography [27], and colorimetry [28] etc., were reported for the successful estimation of H_2O_2. However, the role of electrochemical tools is highly appreciated in this regard. Because, this is associated with better selectivity, improved sensitivity etc. In addition to that, it also favours the on-spot determination of analytes. However, a large overpotential is required for the electrochemical measurement of H_2O_2 at a bare electrode due to the slow kinetics [21]. As a result, much effort has been required to design appropriate electrocatalysts for the estimation of H_2O_2. In order to address the limitations of bare electrodes and improve charge transfer kinetics at the electrode-electrolyte interface, enzyme-dependent electrocatalysts have been introduced [29]. Despite the selectivity, the enzymatic electrodes are associated with certain disadvantages, including their cost, reduced lifetime, poor stability and tedious immobilization methods. Further, the method is complicated and pH and temperature dependent [21]. Furthermore, several non-enzymatic catalysts are found to be useful for the electrochemical analysis of H_2O_2. Nevertheless, among many other sensing methods, a reagent less and non-enzymatic metal free electrochemical method for the measurement of H_2O_2 is a still challenge for practical applications to achieve promising electrochemical performance [30].

In this sense, the goal of this work is to design an electrocatalyst for accurate quantification of H_2O_2. It is inferred from the available literature that there are only a limited number of reports available on 3D-foam-type NDG/GCE. Due to this reason, foam-type NDG is prepared using a hydrothermal route and owing to its finite electrical conductivity, large surface area, high sensitivity, long term stability and excellent binding ability [31]. Therefore, herein we proposed the use of cost effective and highly efficient NDG catalyst material for the accurate determination of H_2O_2. The resulted electrode showed enhanced electrocatalytic activity with a minimal interference from possible other electroactive species with a finite selectivity and sensitivity. The investigation reported in this work can be considered an important element of novelty.

2. Materials and methods

2.1. Chemicals and reagents

From Sigma-Aldrich or Merck, the chemicals, including Graphite, nitric acid, sulfuric acid, sodium nitrate, potassium permanganate, Hexamethylenetetramine (HMTA), hydrochloric acid (HCl) Potassium Nitrate (KNO_3), and Hydrogen Peroxide (H_2O_2), and urea were procured. All the materials are received as such and utilized for conducting the various experiments. Phosphate buffer solution (PBS) with a pH of 7.0 is prepared using Na_2HPO_4 and NaH_2PO_4. At around 30 °C, ambient temperature is used for all electrochemical tests. DI water, which has a resistivity of 18.2 MΩ cm, is utilized as the electrolyte throughout the experiment.

2.2. Preparation of graphene oxide (GO)

Hummers' method is used to prepare GO [32]. In a nutshell, 50 mL of H_2SO_4 and 2.0 g of graphite were combined in a reagent bottle and agitated briskly under ice-cold conditions. Following the addition of 2.0 g of $NaNO_3$ and 6.0 g of $KMnO_4$ to the mixture, the temperature was progressively raised to 35 °C, where the reaction was sustained for a whole day. Consequently, this mixture was diluted using 80 mL DI water and increased to 50 °C. Later 20 ml of H_2O_2 was slowly added to this solution. Finally, the resulting material was toughly eroded with DI up to attain to neutral solution state. This resulting material was vacuum dried at 60 °C for one day and designated as a GO, which was dispersed in deionized water. To achieve the complete dispersion of the solution, it was sonicated for 60 min.

2.3. Synthesis of 3D-foam nitrogen doped graphene (3D-NDG)

The 3D-foam NDG was synthesized as follows: initially, 4.0 g of HMTA, 6.0 g of GO, and 10 ml of ultrapure water were placed in a 30 ml stainless steel autoclave, which was closed tightly. Further, the autoclave was kept in a box furnace and heated to 450 °C for 24 h (with an increase rate of 15 °C/min) and maintained till the solution attained the desired temperature. After 24 h, it was cooled to room temperature. After filtering, the resultant material is thoroughly cleaned three times using H_2O and C_2H_5OH. It is then dried for 2 h at 60 °C in a vacuum oven.

2.4. Electrochemical characterization

An Auto Lab electrochemical interface and Impedance analyser were used with a conventional three-electrode system to perform all electrochemical experiments. Pt, Ag/AgCl (3 M KCl), and modified GCE (0.07 cm^2) are used as the working, counter, and reference electrodes, respectively. To prepare the working electrode (NDG/GCE), firstly, GCE was mirror polished in turn using 0.3, 0.2, and 0.05 μm alumina powders. This was done after completely washing with Milli-Q water and sonicating in DI water for 5 min. To ensure uniform dispersion, an additional 1 mg of synthesized NDG was added to DMF (1 mg/mL). It was gently sonicated. NDG/GCE was then obtained by drop-casting 5 μL of this suspension onto the GCE and letting it air dry to eliminate the solvent. Under the same experimental setup, basic GCE and GO/GCE were created for comparison. Before starting any experiment, argon gas is used to deaerate the reaction mixture.

2.5. Physico-chemical characterization techniques

The Contact angle analysis was carried out with the AST-made VCA Optima XE model, USA. Thermogravimetric analysis (TGA) studies are examined with the model SDT Q600 V8.3 Build 101. The as-synthesised material's surface and morphological characteristics were investigated Using a TESCAN-VEGA3 scanning electron microscope (SEM). A 200 kV Tecnai G20 microscope is used for high-resolution transmission electron microscopy (HR-TEM) examination. Renishaw Invia Raman Microscope, UK, with 18 mW intensity, was employed to carry out the Laser Raman analysis. FT-IR spectra in the transmittance mode were recorded of the synthesised materials using FT-IR spectroscopy (Make: Thermo Electron Corporation; Model: Nexus 670). Through Ni-filtered Cu Kα radiation (λ = 0.15406 nm), the produced materials were subjected to X-ray diffraction (XRD) investigation using a Philips PAN analytical PRO X-ray diffractometer. With a counting period of 15 s per 0.1 and a narrow receiving slit (0.5°), the XRD patterns were acquired using a step-scanning mode. X-ray photoelectron spectroscopy (XPS) analyses were conducted using a Thermo Scientific (UK) Multilab 2000 XPS instrument. A 200 W power Mg Kα X-ray (1253.6 eV) was employed as the exciting source, and data were collected using a 10-eV energy pass. 10^{-10} mbar of vacuum was maintained throughout the experiment. Using the Lorentzian mix product function and Gaussian and Lorentzian background curves, the experimental data were fitted.

3. Results and discussion

3.1. Contact angle measurements

To understand the wettability of synthesised NDG, it was spread on a glass substrate and contact angle measurements were recorded. For the experiment, a fine water droplet of 2 μL was dropped on the surface of NDG, and the syringe was carefully removed from the droplet without any disturbance. The image of the droplet was taken within 60 s using the camera fitted in the device, which was provided in Fig. 1. The measured average contact angle was 130.4°. From the image, it can clearly be understood that NDG was hydrophobic rather than hydrophilic after the 60s it has shown a hydrophilic nature.

3.2. Thermogravimetric analysis

Further, TGA has been carried out to understand the thermal stability of NDG. It was compared with the thermogravimetric profile of graphite. Fig. 2 illustrates the decomposition of graphite, which began at 400 °C and ended at 700 °C. In the case of NDG, the starting decomposition temperature was around 600 °C, and it was completely decomposed at around >800 °C. The TGA analysis confirms that the resulted NDG material have finite thermal stability after nitrogen doping than graphite.

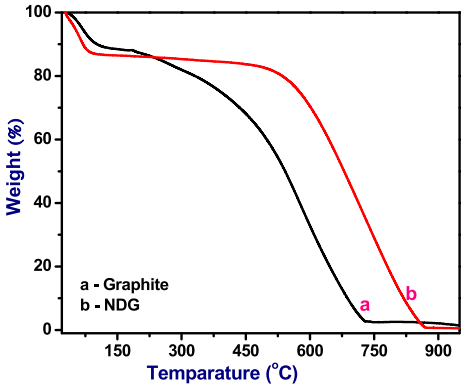

Fig. 2. TGA thermogram of (a) Graphite and (b) NDG.

3.3. Surface morphological studies

To illustrate the surface morphology of NDG, SEM and HR-TEM analysis were carried out and they are shown in Fig. 3. The image reveals wrinkled, disordered, foam type of morphology. It was inferred as one of the physical characteristics of NDG [15]. This results from stronger van der Waals interactions after O2-containing functional groups are removed via the hydrothermal method.

3.4. FT-IR spectroscopic studies

The different functional groups were examined using FT-IR spectroscopic technique. As evidenced in Fig. 4, the band obtained at 2982 cm^{-1} is due to the -C-H vibration of NDG. In addition to a peak that appeared around 1615 $cm^{-1,}$ strongly implying the carbonyl group (-C=O) vibration, which persists at NDG corners. The band observed at 1415 cm^{-1} strongly corresponds stretching vibration of the -C=C- bond [15]. In general, the -C=O group is quickly decreased during heating via the hydrothermal route at higher temperatures; however, NDG exhibits a weak reaction from the -OH group. The peaks that appeared around 1230 cm^{-1} strongly correspond to the -CN function group in the resulting 3D-NDG material. The band observed at 3437 cm^{-1} is attributed to −N=H stretching vibrations.

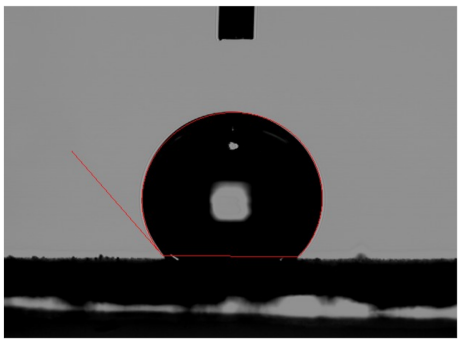

Fig. 1. Contact angle image of NDG on glass substrate.

3.5. Raman spectroscopic analysis

This technique is extensively utilized to This technique is extensively utilized to examine the saturated and unsaturated nature of carbon and its associated materials. Fig. 5 displays the Raman spectra of NDG using graphite materials. It can be seen that two prominent peaks, corresponding to the D and G bands, emerged at 1350 cm^{-1} and 1593 cm^{-1} respectively. These appear due to the presence of carbon materials. These bands are assigned, respectively, to the breathing mode of k-point phonons of A_{1g} symmetry and the E_{2g} phonon of graphitic carbon. The computed I_D/I_G ratio increases from 0.8 to 1.5 in Fig. 5, owing to the formation of smaller graphitic (sp^3) domains and the addition of nitrogen to the carbon network. Eq. (1) was utilized to determine the crystallite size by utilizing the D/G ratio [33].

$$L_a = \left(2.4 \times 10^{-10}\right) \lambda_{laser}^4 \left(I_D/I_g\right)^{-1} \quad (1)$$

Where, L_a - Crystallite size in nm, λ - wavelength in nm. The calculated sizes of GO and NDG materials as 20.1 and 11.4 nm, respectively, which indicates the reduction in the crystallite size after the doping of the Nitrogen element into the carbon network.

3.6. X-ray diffraction (XRD) analysis

Further a non-destructive powerful X-ray diffraction (XRD) technique is used to examine the crystallinity behavious of synthesized materials. The XRD spectrum of synthesised NDG materials is shown in Fig. 6. It showed that a strong diffraction

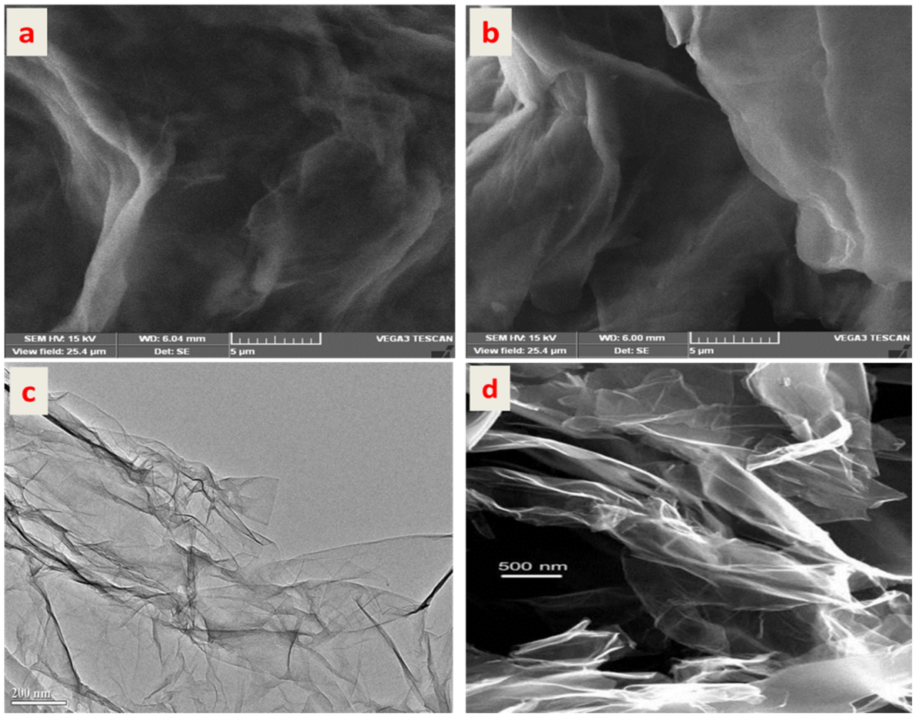

*Fig. 3. **a** & **b** SEM image of 3D foam of NDG. **c** & **d** showed the HR-TEM image of 3D foam of NDG.*

peak observed at a 2θ value of 26.9 corresponds to the crystalline nature of the NDG (002) plane. In addition to this, the small peak found at the 2θ value of 55.02 strongly signifies the (110) plane. The appearance of these diffraction peaks indicates good crystallinity of the material. The interlayer distance of the NDG material was calculated using Braggs equation [Eq. (2)] [34]. In this equation, the interlayer spacing, diffraction angle, order of reflection, and wavelength of the incident X-ray radiation (1.54 Å) are denoted by dd, θ, n, and λ lambda, respectively. The interlayer distance of the NDG material was calculated to be roughly 3.9 Å using this relation.

$$\lambda = 2d\sin(\theta)/n \tag{2}$$

3.7. XPS analysis

Further, the resulted NDG materials was characterized by using XPS technique to examine the presence and nature of the N atom in NDG, as shown in Fig. 7. Fig. 7a demonstrate the different composition of carbon atoms in different functional groups are fitted. The −C−N−, −C−O−, and −C−C− bonding states were identified as the causes of the fitted peaks that were seen at 288.7 eV,

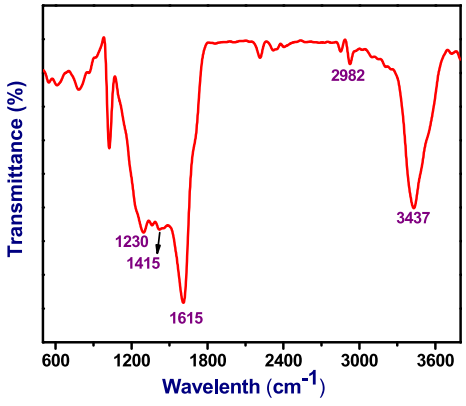

Fig. 4. FT-IR spectra of synthesized NDG material.

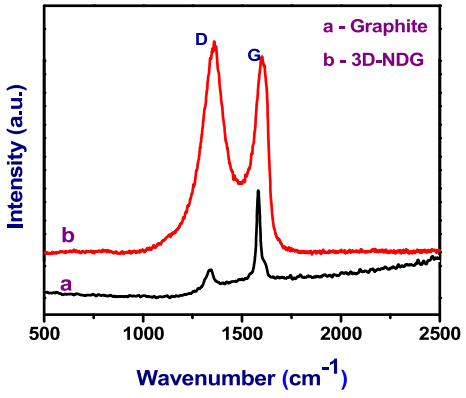

Fig. 5. Laser Raman spectra of (a) Graphite and (b) NDG material.

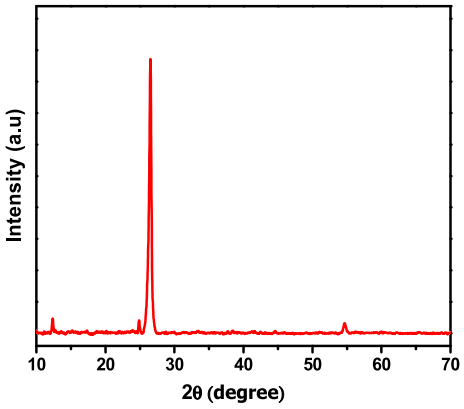

Fig. 6. X-ray diffraction spectra of NDG material.

285.7 eV, and 284.4 eV, respectively. The deconvolution of N1s spectra is fitted into three major peaks observed at 397.9, 398.9, and 400.9 eV, strongly corresponding The pyridinic-N, pyrrolic-N, and quaternary-N species found in the synthesized NDG material were identified as the cause of these peaks. The XPS analysis clearly confirms that nitrogen atom is successfully doped into the carbon network of NDG.

3.8. Electrochemical analysis

Further electrocatalytic property of the synthesized NDG material is examined with the standard outer sphere redox couple. Fig. 8 compares The cyclic voltammetry (CV) profiles of unmodified GCE and NDG/GCE in 5 mM $[Fe(CN)_6]^{3-/4-}$ are shown in Fig. 8. At a 20 mV s^{-1} scan rate, the bare GCE (curve a) displays well-resolved oxidation and reduction peaks with a peak potential difference (ΔEp) of 110 mV. From this analysis, the diffusion coefficient was calculated as 1×10^{-4} cm^2 s^{-1} with the help of the following well-known Randles–Sevcik equation (Eq. (3)).

$$i_p = (2.69 \times 10^5) n^{3/2} A c D^{1/2} \upsilon^{1/2} \quad (3)$$

Where, i_p-Peak current; A-Area of the electrode; C- Concentration of solution used; D-Diffusion coefficient; υ-Scan rate; n-Number of electrons transferred in the reaction. NDG/GCE (curve b) on the other hand, showed higher redox activity than bare GCE, suggesting that the addition of nitrogen improved the electrochemical action of graphene sheets. It can show the ΔE_p as 90 mV along with enhanced redox peak currents. In addition to that, the diffusion coefficient value was also improved to 4.6×10^{-4} cm^2 s^{-1}. However, the capacitive loop is larger when compared to bare GCE. This outcome is consistent with earlier studies [15].

3.9. Electrocatalytic estimation of H_2O_2 using NDG/GCE

A further NDG material is explored towards the electrocatalytic application due to its finite thermal

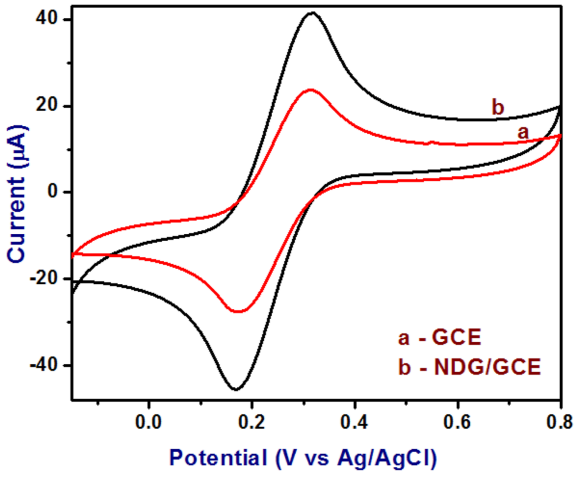

Fig. 8. Shows CV responses of (a) GCE and (b) NDG/GCE in 5 mM of each $[Fe(CN)_6]^{3-/4-}$ containing 0.1 M KNO_3 at a scan rate of 20 mVs^{-1}.

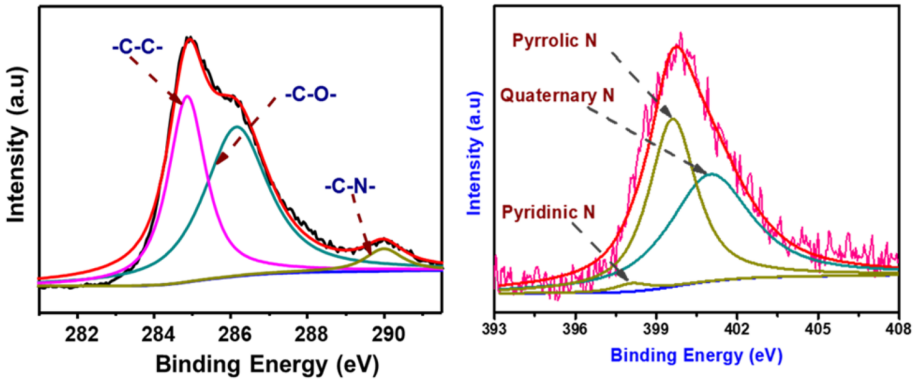

Fig. 7. Showed the high resolution deconvoluted XPS spectra of the (a) C1s (b) N1s spectrum of the synthesized NDG.

and electrical conductivity properties. The CV studies of these electrodes are shown in Fig. 9. Whereas bare GCE and GO/GCE (curve a & curve b) in PBS having 1.5 mM H_2O_2 don't exhibit any significant peak for H_2O_2 reduction, which confirms the lack of electrocatalytic activity due to sluggish electrode kinetics. However, in the case of NDG/GCE (curve c), a reduction peak was observed at an applied overpotential of −0.15 V towards the electrochemical determination of H_2O_2. This observation strongly suggests that NDG possesses faster electron transfer kinetics at the interface and improved catalytic behaviour toward H_2O_2 reduction. Usually, Nitrogen-doped materials have more surface area than undoped graphene materials, which will be echoed in their electrocatalytic behaviour. NDG can afford several active sites due to the defects in it. In addition to that, the disorder and expanded interlayer spacing are found to be effective in trapping the active materials. These features favour the improved electrochemical performance of NDG/GCE towards electrochemical H_2O_2 determination. The obtained irreversible reduction curve at NDG/GCE may be explained by the subsequent Eq. (3) [35].

$$H_2O_2 \rightarrow O_2 + 2H^+ + 2e^- \quad (4)$$

3.10. Amperometric detection of H_2O_2 at NDG/GCE

Amperometric measurement was carried out to assess the sensitivity and limit of detection of NDG for electrochemical H_2O_2 estimation. Fig. 10a shows the amperometric profile of NDG/GCE for the electrochemical determination of H_2O_2. When the experiment was going on, each time successively added 0.5 μM of H_2O_2 in stirred PBS at fixed applied potential of −0.15 V vs. Ag/AgCl. Every addition of

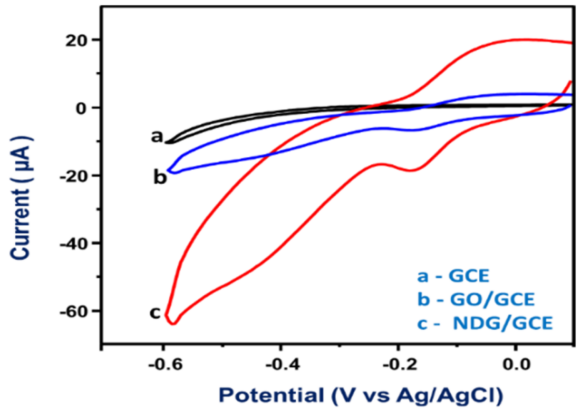

Fig. 9. Cyclic voltammetry of (a) bare GCE, (b) GO/GCE (c) NDG/GCE in 1.5 mM H_2O_2 containing 0.1 M PBS at a scan rate of 20 mV/s.

H_2O_2 leads to the enhancement in the reduction current steeply and the steady-state is attained within less than 3s. A linear variation in sensitivity is observed with increasing H_2O_2 concentration from 0.5 μM to 16 μM, as seen in Fig. 10b; the correlation coefficient (R2) of the calibration plot was 0.99. The electrode's sensitivity and limit of detection (LOD) and limit of quantification (LOQ) were computed as, respectively, 0.3 $\mu A/\mu M^{-1}$ and 0.3 μM, 0.99 μM respectively using the following equations.

Limit of Quantification (LOQ) and Limit of Detection (LOD) estimation:

$$LOD = 3.3 * s_b/m \quad LOQ = 10 * s_b/m$$

Where, sd is the standard deviation of the blank sample and "m" is the slope of the linear calibration plot of H_2O_2 measurement [31].

The acquired results demonstrate a finite activity towards precise H_2O_2 determination and are comparable with other studies, as Table 1 illustrates.

3.11. Interference study

Further, the selectivity of NDG/GCE during the electrochemical determination of H_2O_2 was evaluated using amperometric measurements, which are provided in Fig. 11. 1.5 mM of H_2O_2 was added to the study along with other chemicals that can interfere, such as dopamine, ascorbic acid, SO_4^{2-}, and NO^{3-}. Compared to H_2O_2, the concentration of foreign molecules is two times higher. As can be observed in Fig. 11, the current response due to the interfering molecules is quite negligible, by which it can be concluded that the electrode focuses only on estimating H_2O_2 while other potentially interfering molecules are present.

3.12. Repeatability, reproducibility, and stability studies

Further reproducibility studies of proposed NDG/GCE were carried using five identical NDG/GCEs. These were prepared under similar conditions and performed CV analysis was recorded in the electrolyte of PBS containing 1.5 mM H_2O_2. From the experiment, it is revealed that the relative standard deviation (RSD) in the current response between these electrodes is found to be 2.8 %, which confirms the reproducibility of NDG/GCE. CV was used to test the repeatability of a single NDG/GCE at the same H_2O_2 concentration. Ten consecutive CVs were recorded using single NDG/GCE. From the experiment, it is revealed that RSD in sensitivity was only 1.5 %. For the electrochemical determination of H_2O_2, it can be determined that the

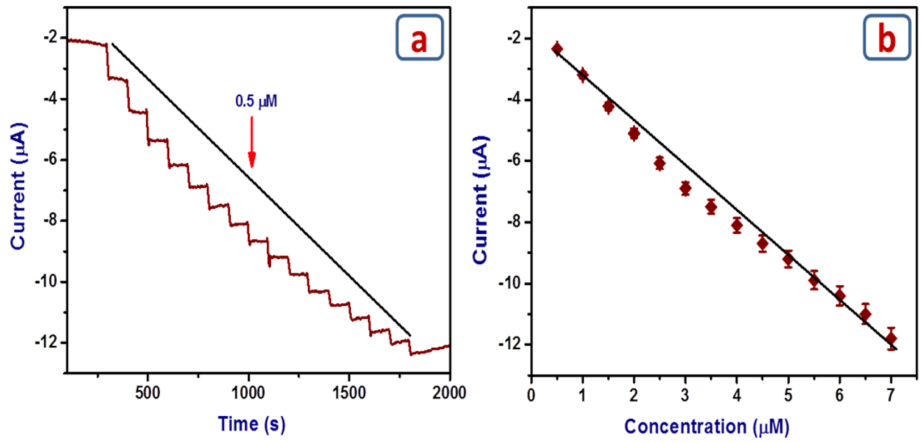

*Fig. 10. **(a)** Typical chronoamperometric response of NDG/GCE for successive addition of 0.5 μM H_2O_2 in 0.1 M PBS (pH 7.0) at applied potential −0.15 V. **(b)** The corresponding calibration plot of Fig. 10a.*

electrode had a stable matrix. To understand the stability of the developed sensor platform followed by it is kept in a desiccator at room temperature. The catalytic activity was intermittently examined for 15 days. From these studies, it is observed that there is no considerable change in current responses concerning the one which is obtained with a 97 % retention rate, as depicted in Fig. 12. In general, it can be established that NDG/GCE shows a better electrochemical performance with good repeatability, reproducibility, and stability.

3.13. Detection of H_2O_2 in real sample analysis

By using the usual addition procedure, we further By using the usual addition procedure, we further extend our investigation to approximate the very low-level concentration of H_2O_2 in an actual sample. Water samples taken from tap water were mixed with a series of different amounts of H_2O_2 and subjected to the CA method for analysis. Table 2 displays the recovery studies that were the outcome. The limited results obtained indicate that the designed sensor system is capable of detecting H_2O_2 at low concentrations. The results have also been

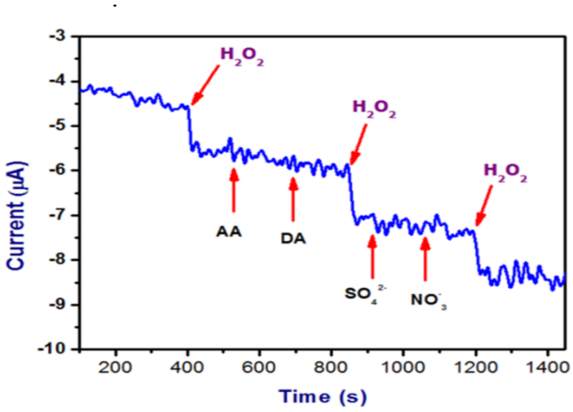

Fig. 11. Chronoamperometric response of successive addition of respective electroactive species on NDG/GCE at −0.15 V in 0.1 M PBS.

Table 1. The analytical performance comparison for previous H_2O_2 electrochemical sensors with the proposed NDG/GCE.

Electrode Materials	Linear Range (μM)	Detection Limit (μM)	References
PEDOT-CuO[a]	40–10,000	8.5	[36]
$CuGa_2O_4$	5–200	5	[37]
LSG-Ag	100–10,000	7.9	[38]
Fe/CV-CPE	20–1100	20	[39]
SS/AuNPs	10–1000	3.97	[40]
NDG/GCE	0.5–16	0.3	Present work

[a] PEDOT-CuO - Poly(3,4-ethylene dioxy thiophene) Copper(II) oxide, $CuGa_2O_4$ - spinel-type $CuGa_2O_4$ nanoparticle-modified glassy carbon electrode, LSG-Ag- laser-scribed graphene decorated with silver nanoparticles, Fe/CV-CPE - carbon paste electrode modified with Fe-exchanged zeolitic volcanic tuff, SS-AuNPs - Stainless steel, gold nanoparticles.

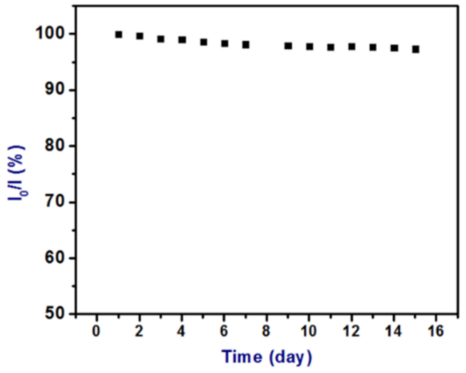

Fig. 12. Long-term stability of NDG/GCE was studied in 1.5 mM H_2O_2 containing PBS for 15 days.

Table 2. Determination of concentration of H_2O_2 in various types of water with proposed NDG/GCE using the CA technique.

Samples	Added (μM)	Found (μM)	Recovery (%)
Sample-1	0.50	0.49	98.0
	1.00	1.02	102.0
	2.00	1.98	99.0
	3.00	3.02	100.6
	4.00	4.02	100.5
Sample-2	0.50	0.51	102.0
	1.00	0.99	99.00
	2.00	2.01	101.5
	3.00	3.02	100.6
	4.00	3.99	99.7

thoroughly verified, and this makes it a useful sensor for the real-time detection of H_2O_2 in a variety of industrial or H_2O_2 containing materials.

4. Conclusions

This work presents an easy way to synthesize nitrogen-doped 3D-foam graphene as a potential electrode material for H_2O_2 electrochemical detection. The surface characteristics of synthesized materials are examined with various spectroscopy and microscopy tools. Using Raman studies, it has been concluded that an increase in the intensity I_D/I_G ratio confirms the successful incorporation of nitrogen in the carbon network. The resulted NDG material have a high surface area, huge number of structural defects/active sites, which contributes to the excellent electrocatalytic response towards H_2O_2. Further, NDG/GCE produces better electrochemical performance, like enhanced reduction current at low overpotential, while the electrochemical determination of H_2O_2 when compared to bare GCE. Further, it exhibited selectivity, linear range, rapid response, stability, and minimal detection limit. Hence, the current procedure is identified as a favourable platform for reagent less, non-enzymatic estimation of H_2O_2. As a result, this process simplifies the large-scale synthesis of NDG for a variety of electrochemical applications.

Ethics information

This work did not involve any human participants, human data, human tissue, or animal experiments. Ethical approval was therefore not required in accordance with institutional and national guidelines.

Funding

This study received no external funding.

Conflicts of interest

The authors declare that they have no competing interests.

Acknowledgements

The authors greatly acknowledge the management of Nanosol Energy Pvt. Ltd, Hyderabad, India, for their constant support and encouragement.

Supporting information

https://kijoms.uokerbala.edu.iq/cgi/editor.cgi?article=3433&window=additional_files&context=home.

References

[1] K. Jasuja, V. Berry, Implantation and growth of dendritic gold nanostructures on graphene derivatives: electrical property tailoring and Raman enhancement, ACS Nano 3 (2009) 2358–2366, https://doi.org/10.1021/nn900504v.
[2] X. Li, J. Yu, S. Wageh, A.A. Al-Ghamdi, J. Xie, Graphene in photocatalysis: a review, Small 12 (2016) 6640–6696, https://doi.org/10.1002/smll.201600382.
[3] S.R. Kanuganti, R. Sultana, D. Kolli, G.K. Maddula, M. R. Singampalli, Facile one-pot synthesis of sulphur doped graphene for non-enzymatic sensing of hydrogen peroxide, Int. J. Environ. Anal. Chem. 103 (2023) 8051–8062, https://doi.org/10.1080/03067319.2021.1980785.
[4] K.P. Loh, Q. Bao, P.K. Ang, J. Yang, The chemistry of graphene, J. Mater. Chem. 20 (2010) 2277–2289, https://doi.org/10.1039/B920539J.
[5] H. Gong, X. Hu, R. Zeng, Y. Li, J. Xu, M. Li, D. Tang, CRISPR/Cas12a-based photoelectrochemical sensing of microRNA on reduced graphene oxide-anchored Bi2WO6 coupling with catalytic hairpin assembly, Sensor Actuator B Chem. 369 (2022) 132307. https://www.sciencedirect.com/science/article/abs/pii/S0925400522009492?via%3Dihub.
[6] M. Sajibul, A. Bhuyan, M.N. Uddin, M.M. Islam, F. A. Bipasha, S.S. Hossain, Synthesis of graphene, Int. Nano Lett. 6 (2016) 65, https://doi.org/10.1007/s40089-015-0176-1.
[7] J. Shu, Z. Qiu, D. Tang, Self-referenced smartphone imaging for visual screening of H_2S using CuxO-polypyrrole conductive aerogel doped with graphene oxide framework, Anal. Chem. 90 (2018) 9691–9694. https://pubs.acs.org/doi/10.1021/acs.analchem.8b03011.
[8] X. Wang, H. You, F. Liu, M. Li, L. Wan, S. Li, Q. Li, Y. Xu, R. Tian, Z. Yu, D. Xiang, Large-scale synthesis of few-layered graphene using CVD, Chem. Vap. Depos. 15 (2009) 53–56, https://doi.org/10.1002/cvde.200806737.
[9] M. Coroş, F. Pogăcean, M.C. Roşu, C. Socaci, G. Borodi, L. Mageruşan, A.R. Biriş, S. Pruneanu, Simple and cost-effective synthesis of graphene by electrochemical exfoliation of graphite rods, RSC Adv. 6 (2016) 2651–2661, https://doi.org/10.1039/C5RA19277C.
[10] A.V. Murugan, T. Muraliganth, A. Manthiram, Rapid, facile microwave-solvothermal synthesis of graphene nanosheets and their polyaniline nanocomposites for energy storage, Chem. Mater. 21 (2009) 5004–5006, https://doi.org/10.1021/cm902413c.
[11] Q. Zhuo, J. Gao, M. Peng, L. Bai, J. Deng, Y. Xia, Y. Ma, J. Zhong, X. Sun, Large-scale synthesis of graphene by the reduction of graphene oxide at room temperature using metal nanoparticles as catalyst, Carbon 52 (2013) 559–564, https://doi.org/10.1016/j.carbon.2012.10.014.

[12] W. Chen, L. Yan, P.R. Bangal, Preparation of graphene by the rapid and mild thermal reduction of graphene oxide induced by microwaves, Carbon 48 (2010) 1146–1152, https://doi.org/10.1016/j.carbon.2009.11.037.
[13] G. Cai, Z. Yu, R. Ren, D. Tang, Exciton-plasmon interaction between AuNPs/Graphene nanohybrids and CdS quantum dots/TiO_2 for photoelectrochemical aptasensing of prostate-specific antigen, ACS Sens. 3 (2018) 632–639. https://doi/10.1021/acssensors.7b00899.
[14] R. Rajaram, J. Mathiyarasu, An electrochemical sensor for homocysteine detection using gold nanoparticle incorporated reduced graphene oxide, Colloids Surf. B Biointerfaces 170 (2018) 109–114, https://doi.org/10.1016/j.colsurfb.2018.05.066.
[15] S. Mutyala, J. Mathiyarasu, A highly sensitive NADH biosensor using nitrogen doped graphene modified electrodes, J. Electroanal. Chem. 775 (2016) 329–336, https://doi.org/10.1016/j.jelechem.2016.06.011.
[16] A.J. Clancy, H. Au, N. Rubio, G.O. Coulter, M.S. Shaffer, Understanding and controlling the covalent functionalisation of graphene, Dalton Trans. 49 (2020) 10308–10318, https://doi.org/10.1039/D0DT01589J.
[17] L. Liu, X. Yan, Y. Zhang, D. Deng, H. He, Y. Lei, X. Shen, L. Luo, Mn3O4–CeO2 hollow nanospheres for electrochemical determination of hydrogen peroxide, ACS Appl. Nano Mater. 6 (2023) 2116–2124, https://doi.org/10.1021/acsanm.2c05123.
[18] M. Xu, Z. Yu, Q. Wei, D. Tang, Probing trace of intracellularly-originated hydrogen peroxide-based Pt-Cd bimetallic nanozyme on an enzyme-free electrochemical sensor, Anal. Chim. Acta 1324 (2024) 343096, https://doi.org/10.1016/j.aca.2024.343096.
[19] M. Borras-Brull, P. Blondeau, J. Riu, The use of conducting polymers for enhanced electrochemical determination of hydrogen peroxide, Crit. Rev. Anal. Chem. 51 (2021) 204–217, https://doi.org/10.1080/10408347.2020.1718482.
[20] Z. Lu, L. Wu, X. Dai, Y. Wang, M. Sun, C. Zhou, H. Du, H. Rao, Novel flexible bifunctional amperometric biosensor based on laser engraved porous graphene array electrodes: highly sensitive electrochemical determination of hydrogen peroxide and glucose, J. Hazard Mater. 402 (2021) 123774, https://doi.org/10.1016/j.jhazmat.2020.123774.
[21] T. Gurusamy, R. Rajaram, R. Murugan, K. Ramanujam, A web of poly (bis benzimidazole atocopper (ii)) around multiwalled carbon nanotubes for the electrochemical detection of hydrogen peroxide, New J. Chem. 46 (2022) 1222–1231, https://doi.org/10.1039/D1NJ04903H.
[22] A. Kasatkin, A. Urakov, Effect of hydrogen peroxide on erythrocyte temperature in vitro, Chem. Biol. Interact. 354 (2022) 109837, https://doi.org/10.1016/j.cbi.2022.10983.
[23] P. Zhao, S. Chen, Y. Liang, Y. Chen, P. Lan, D. Huo, C. Hou, Metalloporphyrin hemin modified carbon nanotube decorated titanium carbide with redox catalytic ability for electrochemical determination of hydrogen peroxide and uric acid, J. Colloid Interface Sci. 628 (2022) 456–466, https://doi.org/10.1016/j.jcis.2022.07.190.
[24] C. Zhang, L. Li, J. Ju, W. Chen, Electrochemical sensor based on graphene-supported tin oxide nanoclusters for nonenzymatic detection of hydrogen peroxide, Electrochim. Acta. 210 (2016) 181–189, https://doi.org/10.1016/j.electacta.2016.05.151.
[25] Y. Jiang, X. Zhao, Q. Wang, Y. Sun, Y. Cao, N. Han, C. Lee, J. Cao, J. Li, W. Si, Facile synthesis of paper-derived porous activated carbon and the electrochemical determination of hydrogen peroxide, J. Electrochem. Soc. 169 (2022) 056510, https://doi.org/10.1149/1945-7111/ac6ae8.
[26] X.S. Chai, Q.X. Hou, Q. Luo, J.Y. Zhu, Rapid determination of hydrogen peroxide in the wood pulp bleaching streams by a dual-wavelength spectroscopic method, Anal. Chim. Acta. 507 (2004) 281–284, https://doi.org/10.1016/j.aca.2003.11.036.
[27] M. Song, J. Wang, B. Chen, L. Wang, A facile, nonreactive hydrogen peroxide (H2O2) detection method enabled by ion chromatography with UV detector, Anal. Chem. 89 (2017) 11537–11544, https://doi.org/10.1021/acs.analchem.7b02831.
[28] B. Zhou, J. Wang, Z. Guo, H. Tan, X. Zhu, A simple colorimetric method for determination of hydrogen peroxide in plant tissues, Plant Growth Regul. 49 (2006) 113–118, https://doi.org/10.1007/s10725-006-9000-2.
[29] M. Sun, G. Shen, Z. Bai, H. Zhang, H. Liu, X. Liang, Electrochemical determination of hydrogen peroxide using a horseradish peroxidase (HRP) modified gold–nickel alloy nanoparticles glassy carbon electrode (GCE), Anal. Lett. 54 (2021) 2565–2573, https://doi.org/10.1080/00032719.2021.1878367.
[30] Y. Yu, M. Pan, J. Peng, D. Hu, Y. Hao, Z. Qian, A review on recent advances in hydrogen peroxide electrochemical sensors for applications in cell detection, Chin. Chem. Lett. 33 (9) (2022) 4133–4145, https://doi.org/10.1016/j.cclet.2022.02.045.
[31] J. Gaidukevic, R. Aukstakojyte, M. Kozłowski, J. Barkauskas, R. Pauliukaite, A simple preparation of N-doped reduced graphene oxide as an electrode material for the detection of hydrogen peroxide and glucose, Electrochim. Acta 446 (2023) 142113, https://doi.org/10.1016/j.electacta.2023.142113.
[32] H. Park, S. Lim, D.D. Nguyen, J.W. Suk, Electrical measurements of thermally reduced graphene oxide powders under pressure, Nanomaterials 9 (2019) 1387, https://doi.org/10.3390/nano9101387.
[33] M.A. Pimenta, G. Dresselhaus, M.S. Dresselhaus, L. G. Cancado, A. Jorio, R. Saito, Studying disorder in graphite-based systems by Raman spectroscopy, Phys. Chem. Chem. Phys. 9 (2007) 1276–1290, https://doi.org/10.1039/B613962K.
[34] C.S.R. Barria, D.M. Fernandes, C. Freire, E.V. Abalos, A. G. Ruiz, I.R. Ramos, Upgrading the properties of reduced graphene oxide and nitrogen-doped reduced graphene oxide produced by thermal reduction toward efficient ORR electrocatalysts, Nanomaterials 9 (2019) 1761. https://www.mdpi.com/2079-4991/9/12/1761.
[35] A.A. Ensafi, M. Jafari–Asl, B. Rezaei, A novel enzyme-free amperometric sensor for hydrogen peroxide based on nafion/exfoliated graphene oxide–Co3O4 nanocomposite, Talanta 103 (2013) 322–329, https://doi.org/10.1016/j.talanta.2012.10.063.
[36] C. Lete, A.M. Spinciu, M.G. Alexandru, J. Calderon Moreno, S.A. Leau, M. Marin, D. Visinescu, Copper (II) oxide nanoparticles embedded within a PEDOT matrix for hydrogen peroxide electrochemical sensing, Sensors 22 (2022) 8252, https://doi.org/10.3390/s22218252.
[37] H. Yin, Y. Shi, Y. Dong, X. Chu, Synthesis of spinel-type CuGa2O4 nanoparticles as a sensitive non-enzymatic electrochemical sensor for hydrogen peroxide and glucose detection, J. Electroanal. Chem. 885 (2021) 115100, https://doi.org/10.1016/j.jelechem.2021.115100.
[38] E. Aparicio-Martínez, A. Ibarra, I.A. Estrada-Moreno, V. Osuna, R.B. Dominguez, Flexible electrochemical sensor based on laser-scribed Graphene/Ag nanoparticles for non-enzymatic hydrogen peroxide detection, Sensor. Actuator. B Chem. 301 (2019) 127101, https://doi.org/10.1016/j.snb.2019.127101.
[39] A. Maicaneanu, C. Varodi, H. Bedelean, D. Gligor, Physical-chemical and electrochemical characterization of Fe-exchanged natural zeolite applied for obtaining of hydrogen peroxide amperometric sensors, Geochemistry 74 (2014) 653–660, https://doi.org/10.1016/j.chemer.2014.02.005.
[40] D. Huo, D. Li, S. Xu, Y. Tang, X. Xie, D. Li, F. Song, Y. Zhang, A. Li, L. Sun, Disposable stainless-steel wire-based electrochemical microsensor for in vivo continuous monitoring of hydrogen peroxide in vein of tomato leaf, Biosensors 12 (2022) 35, https://doi.org/10.3390/bios12010035.